A Numerical Study of the Effect of Upper-Ocean Shear on Flexible Drogued Drifters

T. K. CHERESKIN, P. P. NIILER AND P. M. POULAIN

Scripps Institution of Oceanography, La Jolla, California

(Manuscript received 19 May 1988, in final form 14 July 1988)

ABSTRACT

The shape and slip of freely drifting, two-dimensional, flexible weighted drogues tethered to a surface buoy in a specified upper-ocean velocity profile are examined numerically. A simple analytic solution for a drogue in a linear shear flow, in the limit of small deviations from a straight vertical configuration, is used to identify the parameters of the problem and to predict the functional dependence of the slip and shape of the drogue on those parameters. The numerical computations, using a finite elements static equilibrium model, confirm the functional dependence predicted by the analytic solution and estimate the parametric dependences. However, a linear shear is not the "worst case" shear one needs to design for. In optimizing a drogue for linear shear, one can make use of the symmetry of the velocity profile to minimize the slip. The design problem arises from not knowing a priori the shear for which one is designing (especially since a drogue eventually moves far from its deployment site) and from asymmetric shear (i.e., the "worst case" shear is one with a bias). The final computations examine three different drogue configurations in a series of profiles that model the diurnal cycle of the mixed layer (a diurnal jet) overlying a linear shear. The best design is found to be one that maximizes the drogue over the depth interval of interest, while minimizing the drag area of the tether. The drogue length needs to be larger than the depth interval of interest to account for the rise and tilt of the drogue in shear flow, but not so large that it averages too far outside the interval. For the practical cases considered, a drogue length that was twice the averaging interval gave the best results.

1. Introduction

This study presents the results of a numerical model used to compute the shape and slip of freely drifting, two-dimensional, flexible, weighted drogues that are tethered to a surface buoy in a specified upper-ocean velocity profile. The horizontal velocity shear is two-dimensional, and the forces of gravity and hydrodynamic drag are in static equilibrium. The purpose of the computation is to ascertain what drogue parameters most critically influence the water-following characteristics of long, flexible drogues in strongly sheared flows in the simplest theoretical model. This computation can both guide the choice of design parameters for mixed layer drifters in more complex oceanic conditions and the interpretation of drogue performance data obtained in actual field conditions. The objective is to design and test a drogue and tether configuration that best follows the vertically averaged water velocity over an a priori specified drogue depth interval. The drogue and tether configurations that we examine are also constrained by practical considerations with regard to commonly available materials, construction and ease of deployment. In this simple model, drogue slip will occur both because of the drag on the tether and drogue and because of the tilt and lift of the tether and drogue from a straight vertical configuration.

The slip that we calculate is a lower bound on the slip we expect to see in the ocean where there is a wind-wave field. Under field conditions, wind and surface gravity waves will also produce forces on the surface float that cause slip; in fact these forces may be the dominant cause of slip. Dynamic "lumped mass" models have been used to compute the slip due to a surface wave field (e.g., Dahlen 1986; Chhabra 1976). However, the simplifying assumptions that need to be made about the surface wave velocity field (e.g., single plane wave; no wave breaking) and the dynamics of three-dimensional surface float response are too severe for including wind and wave effects in our model. (See Chhabra et al. 1987 for a simple model of waves, Niiler et al. 1987 for a discussion of the effect of waves and wind on field data interpretation.) Our computation thus models the conditions of static equilibrium in the spirit of setting a theoretical lower bound on the slip expected in the open ocean. Clearly, if a particular drifter design in static equilibrium cannot meet a minimum slip criterion, it will not meet that criterion in dynamic equilibrium in a wind-wave field.

2. Model

The model equations of static equilibrium are outlined in Berteaux (1976) and are identical to those used by Chhabra (1976) in the static limit. Figure 1 is a

Corresponding author address: Dr. Teresa Chereskin, Scripps Institution of Oceanography, A030, University of California, La Jolla, CA 92093

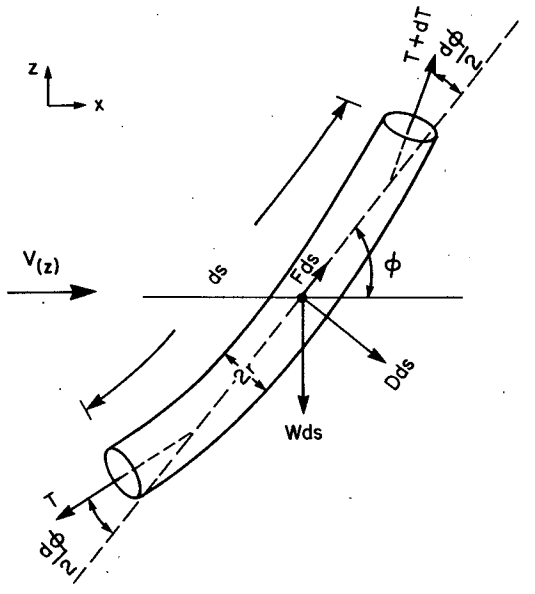

FIG. 1. Definition sketch of balance of forces on a line element.

definition sketch of the forces acting on a line or drogue element of length ds and radius r. The line element is oriented at an angle ϕ with respect to the relative flow velocity vector V, $d\phi$ is the change in angle over the element length. The forces acting on the line element are the tension T, the normal pressure drag Dds, the tangential friction drag Fds and the gravitational force Wds. The change in tension over the element is dT. The equation of static equilibrium for the forces acting normal to the line element is

$$(2T + dT)\sin\left(\frac{d\phi}{2}\right) - Dds - W\cos\phi ds = 0. \quad (2.1)$$

The balance of tangential forces is

$$dT\cos\left(\frac{d\phi}{2}\right) - W\sin\phi ds + Fds = 0 \quad (2.2)$$

where

$$Dds = \rho r C_{DN} V_N^2 ds$$

$$Fds = \pi\rho r C_{TN} V_T^2 ds$$

$$V_N = V\sin\phi, \quad V_T = V\cos\phi$$

and where ρ is the water density, C_{DN} is the coefficient of normal drag, V_N is the component of relative velocity normal to the element, C_{DT} is the tangential drag coefficient, V_T is the component of relative tangential flow, and W is the unit weight in water of the element.

We can assume $d\phi$ is small if we use many elements to approximate the continuous flexible line (tether and drogue), and the equations simplify to

$$d\phi = (D + W\cos\phi)ds/T \quad (2.3)$$

$$dT = (W\sin\phi - F)ds. \quad (2.4)$$

The integral boundary conditions are

$$D_{BH} + D_{EH} + \int_{s_L}^{s_0} (D_H + F_H)ds = 0 \quad (2.5)$$

$$\int_{s_L}^{s_0} ds = L \quad (2.6)$$

where D_B and D_E are the drag on the surface buoy and end weight respectively, s_L and s_0 are the line coordinates at depths Z_L and 0 respectively, and subscript "H" denotes the horizontal component of force. The L is the total line length of the drifter (length of tether and drogue). Equation (2.5) states the condition that the drifter experience no net force when in static equilibrium. Equation (2.6) states that the shape assumed by the drifter in static equilibrium is constrained by the length of the drifter.

3. Method of solution

a. Iteration method

To find the shape of the drifter, we divide the line into many elements and integrate equations (2.3)–(2.6) starting at the (unknown) drifter line endpoint Z_L where the tension T_1 and the angle ϕ_1 are determined from the horizontal and vertical balance of forces on the first element at depth Z_L:

$$(T_1 + F_1 ds)\cos\phi_1 + D_1\sin\phi_1 ds = 0$$

$$(T_1 + F_1 ds)\sin\phi_1 = D_1\cos\phi_1 ds + W_E + Wds.$$

The location of the drifter endpoint is at $x_1 = 0$, $z_1 = Z_L$. To solve for the drifter shape we use the recursion:

$$x_{i+1} = x_i + \Delta x_i, \quad \Delta x_i = ds\cos\phi_i$$

$$z_{i+1} = z_i + \Delta z_i, \quad \Delta z_i = ds\sin\phi_i$$

$$T_{i+1} = T_i + \Delta T_i$$

$$\phi_{i+1} = \phi_i + \Delta\phi_i$$

for $i = 2, N$ where N is the number of segments and where ΔT_i and $\Delta\phi_i$ are calculated from the finite difference approximations to equations (2.3) and (2.4). The drag forces D, F are calculated using the specified velocity profile (linearly interpolated to the depth of the segment midpoint) and the specified drag area distribution as a function of s. In the drag force computation, the velocity V is the flow relative to the drifter; it is the flow velocity minus the mean drifter speed U (assumed to be in the same vertical plane).

An initial guess is made for Z_L and U: the initial Z_L is $L/2$ (the midpoint of the possible depth range) and the initial U is the mean velocity over the depth interval (the velocity at the midpoint if the shear is linear). The solution must satisfy the integral boundary conditions (2.5)–(2.6). These conditions are formulated as minimizations and a binary search based on a double min-

imization procedure is used to iterate on Z_L and U and converge to a solution (Press et al. 1986).

The model resolution depends on the finite element length ds and on the tolerance for the integration of equation (2.5). The finite element length determines the uncertainty in the shape; hence, the uncertainty in the drogue's vertical rise is bounded by ds. The force balance condition (2.5) is specified as a tolerance on the residual force. The residual force can be related to an uncertainty in the drifter speed U and hence the slip. For the solutions discussed in section 5 we used segment lengths of 2.5 cm and a tolerance on the residual force balance of 10^{-6} Newtons, corresponding to a rise accuracy of 2.5 cm and a slip accuracy of 0.1 cm s^{-1}. Smaller tolerances will, of course, increase the model resolution and the accuracy of the solution. However, for comparison with field measurements the chosen tolerance and accuracy are probably at the limit of what can be measured.

b. Relaxation method

An alternative numerical method for finding the shape of the drifter is to integrate equations (2.3) and (2.4) from the surface where the buoyancy $P(0)$ of the surface float is unknown to the bottom of the drogue where the end weight W_E is prescribed. The horizontal and vertical balance of forces on the top element are used to determine the initial angle and tension.

An initial guess is needed for $P(0)$, $\phi(s)$ and U; the initial value of $P(0)$ is W_E, the initial drifter shape is vertical, and the initial U is the mean velocity over the depth interval.

Once the integration is performed and the new angle and tension distributions are calculated, the new mean drifter speed is estimated by a relaxation technique based upon the integrated horizontal forces (2.5):

$$U_{i+1} = U_i + dt\left[D_{BH} + D_{EH} + \int_{s_L}^{s_0} (D_H + F_H)ds\right]$$

where dt is a relaxation coefficient corresponding to a pseudo-time step.

Next, the top buoyancy is computed by relaxation using the integrated vertical force balance:

$$P_{i+1}(0) = P_i(0) + dt'\left[D_{BV} + D_{EV} + \int_{s_L}^{s_0} (D_V - F_V + W)ds\right]$$

with subscript V denoting the vertical component of force and with a new relaxation coefficient dt'. The integration and relaxation methods are applied until the integrated horizontal and vertical forces are smaller than a given tolerance.

Both iteration (A) and relaxation (B) methods were compared for various drifter configurations and gave the same results within the uncertainties. This shows the stability of the results with respect to the specific structure of the numerical methods adopted. The iteration method was applied for the numerical experiments discussed in sections 5 and 7.

4. Design parameters for a holey sock

In constant shear flow there are three primary nondimensional parameters that govern the slip of a simple tethered and weighted holey sock drifter,

drag area ratio:

$$R = C_{D1}d_1h_1/C_{D2}d_2h_2 \tag{4.1}$$

drag-to-weight ratio:

$$\Gamma = 0.5\rho C_{D1}d_1h_1(\Delta V)^2/W_E \tag{4.2}$$

aspect ratio:

$$\lambda = h_2/h_1 \tag{4.3}$$

where ΔV is the horizontal velocity difference across the drogue, C_{Di}, d_i, h_i denote the normal drag coefficient, diameter and length of the drogue ($i = 1$) and tether ($i = 2$), and W_E is the weight on the bottom of the drogue. For the sake of simplicity in this dialogue, the drogue and tether are assumed to be neutrally buoyant, but in practice no additional complications result if other weights or buoyancy elements are added. Tangential drag and lift are not considered.

To obtain the functional dependence of the slip on these parameters, an analytic solution for a two lumped mass system can be obtained in the limit of small amplitude deviations of the drifter from a straight vertical configuration and small slip compared to the velocity difference across the drogue. These small perturbation conditions are also the desired conditions for the drifter performance shape.

In the lumped mass system, we model the drifter as two weightless rigid elements in constant shear flow, as diagrammed on Fig. 2. The vertical and horizontal force balances on the drogue are, respectively,

$$W_E + 0.5\rho(\cos\phi_1)^2 \sin\phi_1 \int_0^{h_1} C_{D1}d_1 |V| V ds_1 = T_2 \cos\phi_2 \tag{4.4}$$

$$0.5\rho(\cos\phi_1)^3 \int_0^{h_1} C_{D1}d_1 |V| V ds_1 + T_2 \sin\phi_2 = 0. \tag{4.5}$$

The horizontal force balance on the tether is

$$0.5\rho(\cos\phi_2)^3 \int_0^{h_2} C_{D2}d_2 |V| V ds_2 - T_2 \sin\phi_2 = 0. \tag{4.6}$$

The torque balance around the bottom of the drogue yields the fourth equation required for the solution for four unknowns: T_2, ϕ_1, ϕ_2, and slip u,

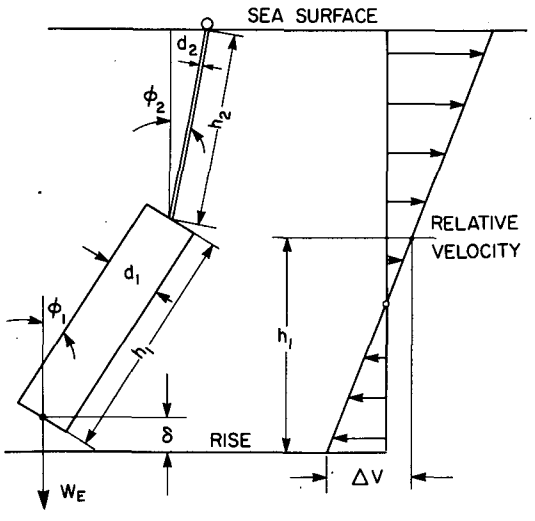

FIG. 2. Definition sketch of 2 lumped mass problem with tether and drogue modelled as rigid elements.

$$T_1 h_1 \sin\phi_2 \cos\phi_1 - T_1 h_1 \cos\phi_2 \sin\phi_1 + 0.5\rho(\cos\phi_1)^2 \int_0^{h_1} C_{D1} d_1 |V| V s_1 ds_1. \quad (4.7)$$

In the above, V is the horizontal velocity relative to the drifter. It is a linear function of both the slip u and the displacement δ of the bottom of the drifter from the equilibrium configuration. In terms of the parameters of the configuration on Fig. 2,

$$\delta = h_2(1 - \cos\phi_2) + h_1(1 - \cos\phi_1) \quad (4.8)$$

$$V = (\Delta V/h_1)(z - 0.5h_1) - u \quad (4.9)$$

$$s_1 = (z - \delta)/\cos\phi_1 \quad (4.10)$$

$$s_2 = (z - \delta - h_1 \cos\phi_1)/\cos\phi_2 \quad (4.11)$$

and z is measured from the bottom of the drogue in vertical configuration. Note that u defined by (4.9) differs from the drifter speed U of section 2; u is the slip with respect to the flow velocity at the center of the drogue.

In the small amplitude shape deviation, $\sin\phi_i \approx \phi_i$ and $\cos\phi_i \approx 1 - \phi_i^2/2$. In the same approximation, we obtain the expression for slip u from the sum of the horizontal forces [sum of (4.5) and (4.6)], and using (4.8)–(4.11),

$$u/\Delta V = \delta/h_1 - 0.25\phi_1^2 + 0.5R^{-1}(1 + 2\lambda + 4\lambda^2/3). \quad (4.12)$$

First, note that the slip u is proportional to ΔV. Second, the first term on the right hand side is due to the rise of the drogue in shear; the second is due to the tilt; the third is due to the drag of the tether. From (4.5) and (4.12) the expressions for δ and ϕ_2 are

$$\delta/h_1 = 0.5(\phi_1^2 + \phi_2^2) \quad (4.13)$$

$$\phi_2 = 0.25\Gamma R^{-1}(1 + 2\lambda + 4\lambda^2/3) \quad (4.14)$$

and from (4.7) the expression for ϕ_1 is

$$\phi_1 = \Gamma/32 + \Gamma(8R)^{-1}(1 + 2\lambda + 4\lambda^2/3) \quad (4.15)$$

The second term is a condition from the tilt of the tether. All these expressions are valid for $R \gg 1$, $\Gamma \ll 1$ and $\lambda \sim O(1)$. Since in typical design, $\lambda \approx 1$, and if $R \gg 16$, then the tilt and rise is due to the drogue only and the tether is practically vertical in comparison.

This analysis shows that firstly, for a distributed drogue in shear, the slip u is proportional to ΔV and inversely proportional to R, and directly proportional to $(\Gamma/32)^2$. Thus, adding weight very quickly reduces the slip, as W_E^{-2}, and increasing the drag area ratio R reduces the slip as R^{-1}. In contrast, for a highly concentrated drogue drag element in shear, the slip would decrease as $R^{-0.5}$. In the next section we use the fully nonlinear model to examine the functional dependence of slip predicted by this simple two lumped mass solution over a range of parameters.

5. Numerical results

The numerical model equations were integrated for a range of linear shear [5, 10, 20 × 10^{-2} s^{-1}], drag area ratios R = [10, 20, 50, 100] and end weights [0.5, 1.0, 3.0, 5.0 10.0 kg]. The drifter consists of a 10 m holey sock drogue and a 10 m tether (λ = 1). The diameter of the tether was fixed at 0.0127 m (0.5 in.); the diameter of the sock was varied over the range [0.127 m (5 in.), 0.254 m (10 in.), 0.635 m (20 in.), 1.270 m (50 in.)]. The normal drag coefficient was the same for both the tether and the drogue, C_{Di} = 1.4; the tangential drag coefficient of the drogue was twice that of the tether to account for both sides of the sock being wetted ($C_{T1} = 0.06C_D$, $C_{T2} = 0.03C_D$). The sock and tether were assumed to be neutrally buoyant. Solutions were computed using 800 segments for the integration (2.5 cm resolution).

The 60 numerical solutions were used to examine the parameter dependence of drogue slip and rise derived in the previous section in the limit of λ = 1, $R \gg 1$, and $\Gamma \ll 1$. Figure 3 is a linear regression of slip scaled by shear across the drogue, $u/\Delta V$, versus R^{-1} for $\Gamma < 1$. The number of solutions in this parameter range is 31, although only four independent points are apparent on Fig. 3 because of the scaling of u by ΔV. For fixed values of R, Fig. 4 illustrates how well the sllip scales with the velocity shear across the drogue. In the range of values of Γ that we consider (less than 1), there is very weak dependence on Γ; the line for each value of R includes as many as five different Γ values at each of the three ΔV values, but the dependence is primarily u as a linear function of ΔV.

The linear fit in Fig. 3 suggests $u/\Delta V$ scales as $1.54R^{-1}$ for $\Gamma < 1$. From equation (4.12) for the 2 lumped mass system we calculate a scaling of $2.17R^{-1}$ for λ = 1, neglecting other terms in the equation. The

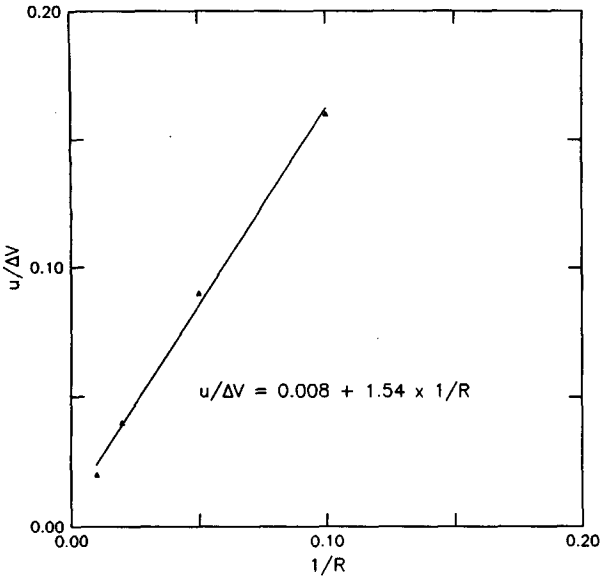

FIG. 3. Slip u scaled by velocity difference across the drogue (ΔV) versus the tether-to-drogue drag area ratio R^{-1}.

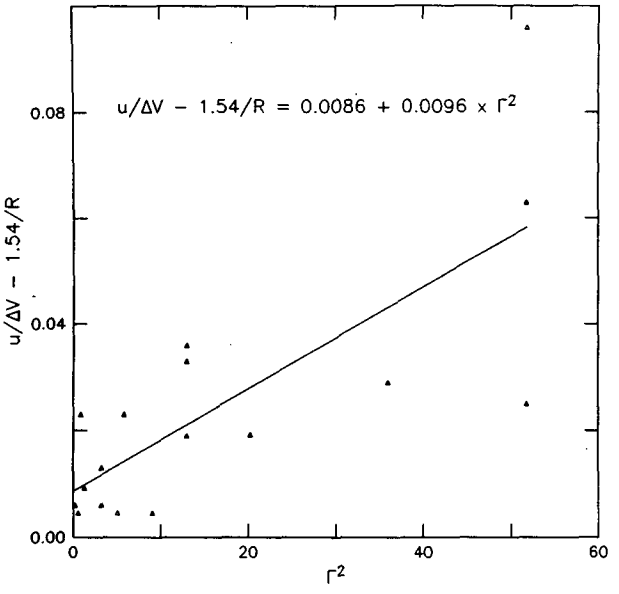

FIG. 5. Slip u scaled by velocity difference across the drogue (ΔV) minus $1.54R^{-1}$ versus the drag-to-weight ratio squared, Γ^2.

flexible distributed drogue modeled numerically verifies the functional dependence of equation (4.12) although the predicted slip is 70% less than that predicted by the simplistic 2 rigid elements, lumped mass solution (after all, the drogue and tether are curved). If we remove the R^{-1} dependence from $u/\Delta V$, we expect the residual to scale as Γ^2 since δ/h_1 and ϕ^2 scale as Γ^2. For values of $R \gg 1$, Fig. 5 shows the results of such a regression. We require $R \gg 1$ since δ and ϕ^2 have a R^{-1} dependence as well. We also need Γ to be small for the lumped parameter solution to be valid, yet we want to look at the Γ dependence so we choose $\Gamma \sim O(1)$. There is a linear trend to the data, although the scatter is great and the regression coefficient is small. This does not show that the slip is unrelated to $\Gamma^2(W_E{}^{-2})$, but rather that in the limit for which the lumped parameter solution is valid that the slip is more influenced by the drag area ratio than by the drag to weight ratio. Slip due to drogue rise occurs at large values of Γ, but the drogue rise quickly reaches a limiting value as Γ is decreased (more weight is added). An end weight of 10 kg was sufficient in all cases, including the largest diameter sock and the strongest shear, to minimize the vertical rise of the drogue. Further reduction in slip can then be achieved by increasing the drag area ratio: either increasing the sock diameter or decreasing the tether diameter.

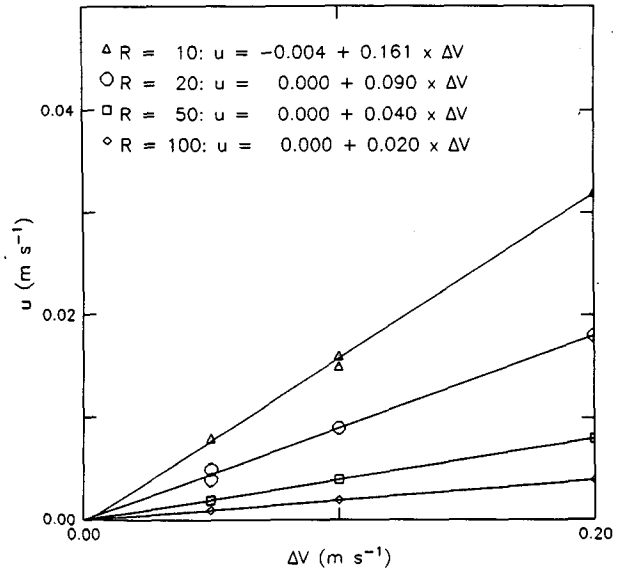

FIG. 4. Slip u versus velocity difference across the drogue (ΔV) at fixed values of the drogue-to-tether drag area ratio R.

6. Design criteria for realistic shear

In the previous two sections we have discussed the behavior of flexible drogued drifters in linear shear flow. The case of linear shear allows us to solve, within certain parameter ranges, the lumped-mass problem analytically and to determine the functional dependence of the parameters of the problem in those limits. The numerical method of solution is not restricted to linear shear profiles or to the parameter ranges already considered. Although linear shear is often a good approximation to observed shears, it is probably not the "worst case" that one needs to design for. Because of the symmetry of the relative velocity profile in the case of linear shear, the drag forces nearly cancel and the slip is dominated by the residual unbalanced forces such as the drag on the surface float and the tether. If one knew a priori that one was designing a drogue to be used in a

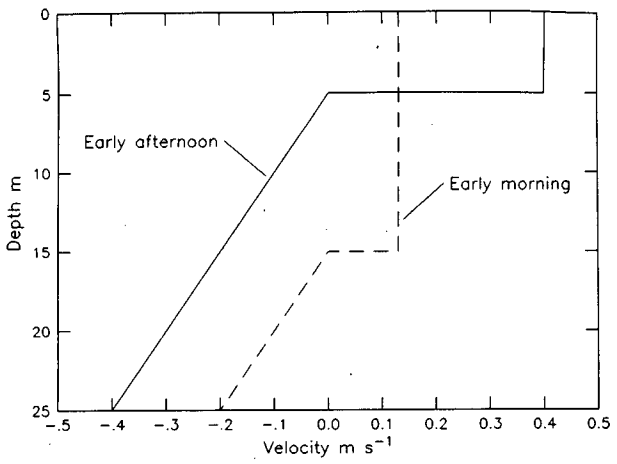

FIG. 6. Step velocity profile (jet) overlying linear shear. The two steps contain the same momentum, 2 $m^2 s^{-1}$. The shallow layer depth (5 m) and large velocity difference (0.4 m s^{-1}) represent the mixed layer in the early afternoon when diurnal heating has re-stratified the mixed layer and confined the layer's momentum to a smaller depth interval, resulting in a diurnal jet. The large layer depth (15 m) and small velocity difference (0.13 m s^{-1}) represents the mixed layer just before dawn when nighttime convective mixing has mixed the layer (and the momentum) down to its maximum depth. The linear shear below the step is identical in these 2 profiles, 0.02 s^{-1}.

linear shear flow, the design guidelines would be straightforward: minimize the cross-sectional area of the float and the diameter of the tether and, within practical considerations, maximize the diameter of the drogue. With regard to the aspect ratio (length of the tether to length of the drogue) one wants to concentrate the drogue at the depth or depth interval of interest (but the drogue must be long enough to take account of its rise in shear flow). Alternatively, if one knew a priori that the shear was linear, a simple rope drogue could be used with length such that on average there was no net drag in the expected shear flow. Obviously, the design problem arises from not knowing, a priori, the flow for which we are designing, especially since a drifter will eventually move far from its deployment site. Our aim, then, is to design for a "worst case" shear. We argue that the worst case shears are those that give rise to a bias. Linear shear and shear due to internal waves should average out over the entire length of the drifter. In the upper ocean, the diurnal jet associated with the daily cycle is a large source of a bias shear. Even in equatorial regions, where the strong shear above the core of the equatorial undercurrent can be approximated by linear shear, the upper 25 meters shows a striking example of a diurnal jet. The Tropic Heat measurements at 0°, 140°W revealed a marked diurnal cycle in both shear (of order 0.01 s^{-1}) and buoyancy frequency but a nearly constant Richardson number (Chereskin et al. 1986).

The shear we chose for the numerical solutions discussed in this section were motivated by these Tropic Heat measurements and mixed layer studies that indicate the presence of a near surface diurnal jet and a nearly constant Richardson number. The model profile consisted of a velocity step (at depths of 5, 10, 15 m) and a linear shear beneath the step (shears of 5, 10, 15, 20 × 10^{-2} s^{-1}). For each case, three different values of momentum were considered (0.5, 1.0, 2.0 $m^2 s^{-1}$), resulting in a total of 36 different velocity profiles. The velocity difference across the step is equal to the momentum divided by the step depth. Thus, the three increasing step depths for a fixed value of momentum represent momentum conservation during the diurnal cycle of the mixed layer, which we expect to observe as the layer depth changes. For a given momentum value, the deepest mixed layer has the smallest velocity change across the step. Figure 6 shows the velocity profile in the beginning of the afternoon when the layer is shallowest and before sunrise when the layer is deepest.

TABLE 1. 5 m sock; 12.5 m tether.

Step (m)	Momentum ($m^2 s^{-1}$)	Shear (s^{-1})	Slip (m s^{-1})	⟨Slip⟩ (m s^{-1})	Lift (m)
5	0.5	0.005	−0.011	−0.011	0.017
5	0.5	0.010	−0.012	−0.012	0.017
5	0.5	0.015	−0.013	−0.013	0.017
5	0.5	0.020	−0.015	−0.015	0.017
5	1.0	0.005	−0.020	−0.020	0.017
5	1.0	0.010	−0.021	−0.021	0.017
5	1.0	0.015	−0.022	−0.022	0.017
5	1.0	0.020	−0.023	−0.023	0.034
5	2.0	0.005	−0.037	−0.037	0.034
5	2.0	0.010	−0.040	−0.040	0.051
5	2.0	0.015	−0.041	−0.041	0.060
5	2.0	0.020	−0.044	−0.044	0.128
10	0.5	0.005	−0.005	−0.005	0.017
10	0.5	0.010	−0.004	−0.004	0.017
10	0.5	0.015	−0.005	−0.005	0.017
10	0.5	0.020	−0.005	−0.005	0.017
10	1.0	0.005	−0.010	−0.010	0.017
10	1.0	0.010	−0.009	−0.009	0.017
10	1.0	0.015	−0.009	−0.009	0.017
10	1.0	0.020	−0.009	−0.009	0.017
10	2.0	0.005	−0.021	−0.021	0.017
10	2.0	0.010	−0.021	−0.021	0.017
10	2.0	0.015	−0.019	−0.019	0.017
10	2.0	0.020	−0.019	−0.019	0.034
15	0.5	0.005	−0.013	−0.002	0.017
15	0.5	0.010	−0.010	−0.002	0.017
15	0.5	0.015	−0.006	−0.001	0.017
15	0.5	0.020	−0.003	−0.001	0.017
15	1.0	0.005	−0.030	−0.003	0.017
15	1.0	0.010	−0.027	−0.004	0.017
15	1.0	0.015	−0.024	−0.003	0.017
15	1.0	0.020	−0.020	−0.003	0.017
15	2.0	0.005	−0.064	−0.007	0.034
15	2.0	0.010	−0.061	−0.007	0.034
15	2.0	0.015	−0.057	−0.007	0.034
15	2.0	0.020	−0.054	−0.007	0.034

TABLE 2. 10 m sock; 10 m tether.

Step (m)	Momentum ($m^2 s^{-1}$)	Shear (s^{-1})	Slip ($m s^{-1}$)	⟨Slip⟩ ($m s^{-1}$)	Lift (m)
5	0.5	0.005	−0.004	−0.004	0.020
5	0.5	0.010	−0.003	−0.003	0.020
5	0.5	0.015	−0.004	−0.004	0.039
5	0.5	0.020	−0.005	−0.005	0.156
5	1.0	0.005	−0.009	−0.009	0.020
5	1.0	0.010	−0.007	−0.007	0.039
5	1.0	0.015	−0.007	−0.007	0.078
5	1.0	0.020	−0.008	−0.008	0.176
5	2.0	0.005	−0.023	−0.023	0.039
5	2.0	0.010	−0.019	−0.019	0.068
5	2.0	0.015	−0.017	−0.017	0.146
5	2.0	0.020	−0.018	−0.018	0.313
10	0.5	0.005	−0.001	−0.001	0.020
10	0.5	0.010	−0.001	−0.001	0.020
10	0.5	0.015	−0.001	−0.001	0.039
10	0.5	0.020	−0.002	−0.002	0.117
10	1.0	0.005	−0.004	−0.004	0.020
10	1.0	0.010	−0.003	−0.003	0.020
10	1.0	0.015	−0.002	−0.002	0.039
10	1.0	0.020	−0.003	−0.003	0.117
10	2.0	0.005	−0.011	−0.011	0.020
10	2.0	0.010	−0.007	−0.007	0.039
10	2.0	0.015	−0.006	−0.006	0.078
10	2.0	0.020	−0.006	−0.006	0.156
15	0.5	0.005	−0.010	0.002	0.020
15	0.5	0.010	−0.002	0.006	0.020
15	0.5	0.015	0.005	0.010	0.039
15	0.5	0.020	0.013	0.015	0.039
15	1.0	0.005	−0.027	0.000	0.039
15	1.0	0.010	−0.020	0.004	0.039
15	1.0	0.015	−0.013	0.007	0.078
15	1.0	0.020	−0.006	0.011	0.117
15	2.0	0.005	−0.061	−0.004	0.156
15	2.0	0.010	−0.055	−0.001	0.234
15	2.0	0.015	−0.050	0.001	0.352
15	2.0	0.020	−0.044	0.003	0.469

The largest velocity change (5 m step and 2 $m^2 s^{-1}$ momentum value) is 0.4 m s^{-1}, corresponding to an extremely large shear value, $80 \times 10^{-2} s^{-1}$. Using these velocity profiles, the numerical model was solved for the shape and slip of three different holey sock drogues, each of which was designed to measure the flow at 15 m. The three sock lengths considered were 5, 10, 15 m with corresponding tether lengths of 12.5, 10, 17.5 m. If no shear is present, the drogue and tether hang vertically with the drogue center at 15 m depth. The diameter of the sock was 1.0 m; the diameter of the tether was 0.004 m (5/32 in. wire). The drag coefficients were the same as those specified in section 5. An end weight of 6.0 kg and a surface float with area 0.06 m^2 were specified. The surface float corresponded to an 11 in. sphere that was submerged 100% of the time; its drag coefficient is 0.5. Since there is a surface jet, a considerable proportion of the slip is due to the drag on the surface float. However, the aim of this calculation is a "worst case" realization, and we are still neglecting surface waves and windage.

Tables 1–3 summarize the slip velocity and the vertical rise of the drogues for the 36 velocity profiles. "Slip" in the tables is the difference between the speed of the drogued drifter and the velocity of the water at 15 m. "⟨Slip⟩" (with angle brackets) denotes the difference between the speed of the drifter and the vertically averaged flow at 15 m. The flow was averaged over 5 m centered at 15 m. The two definitions of slip yield identical results when the averaging interval lies totally within the linear shear part of the profile. When the step profile cuts across upper part of the drogue (within the averaging interval), the estimates of ⟨slip⟩ are substantially less than the unaveraged slips calcu-

TABLE 3. 15 m sock; 7.5 m tether.

Step (m)	Momentum ($m^2 s^{-1}$)	Shear (s^{-1})	Slip ($m s^{-1}$)	⟨Slip⟩ ($m s^{-1}$)	Lift (m)
5	0.5	0.005	−0.002	−0.002	0.022
5	0.5	0.010	−0.002	−0.002	0.132
5	0.5	0.015	−0.006	−0.006	0.571
5	0.5	0.020	−0.014	−0.014	1.252
5	1.0	0.005	−0.004	−0.004	0.022
5	1.0	0.010	−0.004	−0.004	0.176
5	1.0	0.015	−0.007	−0.007	0.615
5	1.0	0.020	−0.016	−0.016	1.318
5	2.0	0.005	−0.014	−0.014	0.066
5	2.0	0.010	−0.011	−0.011	0.308
5	2.0	0.015	−0.013	−0.013	0.747
5	2.0	0.020	−0.024	−0.024	1.582
10	0.5	0.005	−0.014	−0.014	0.044
10	0.5	0.010	−0.013	−0.013	0.308
10	0.5	0.015	−0.015	−0.015	0.791
10	0.5	0.020	−0.023	−0.023	1.494
10	1.0	0.005	−0.032	−0.032	0.264
10	1.0	0.010	−0.033	−0.033	0.747
10	1.0	0.015	−0.038	−0.038	1.450
10	1.0	0.020	−0.048	−0.048	2.197
10	2.0	0.005	−0.070	−0.070	1.582
10	2.0	0.010	−0.080	−0.080	2.461
10	2.0	0.015	−0.092	−0.092	3.252
10	2.0	0.020	−0.108	−0.108	4.043
15	0.5	0.005	−0.006	0.006	0.022
15	0.5	0.010	0.005	0.013	0.088
15	0.5	0.015	0.016	0.021	0.176
15	0.5	0.020	0.026	0.028	0.352
15	1.0	0.005	−0.023	0.003	0.088
15	1.0	0.010	−0.013	0.010	0.220
15	1.0	0.015	−0.004	0.016	0.439
15	1.0	0.020	0.005	0.021	0.703
15	2.0	0.005	−0.059	−0.002	0.615
15	2.0	0.010	−0.052	0.002	0.967
15	2.0	0.015	−0.046	0.005	1.318
15	2.0	0.020	−0.041	0.006	1.670

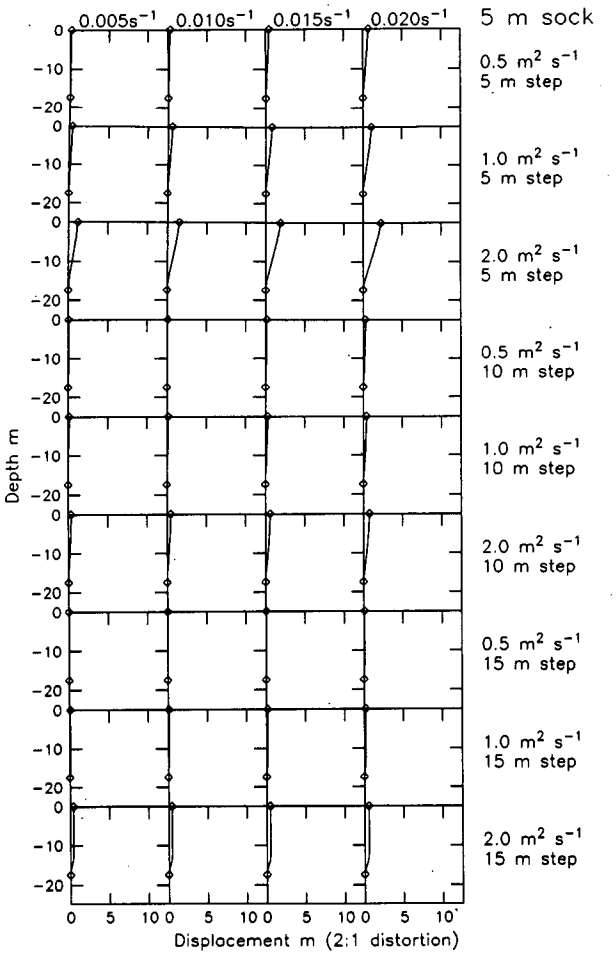

FIG. 7. Shape (horizontal versus vertical displacement from straight vertical) of the 5 m sock corresponding to the solutions in Table 1. Each column corresponds to a fixed value of linear shear. Each row corresponds to a fixed step size and momentum value. The first row corresponds to the first group of solutions in Table 1, etc. The horizontal to vertical distortion is 2:1. The top and bottom of the drogue are marked by open symbols.

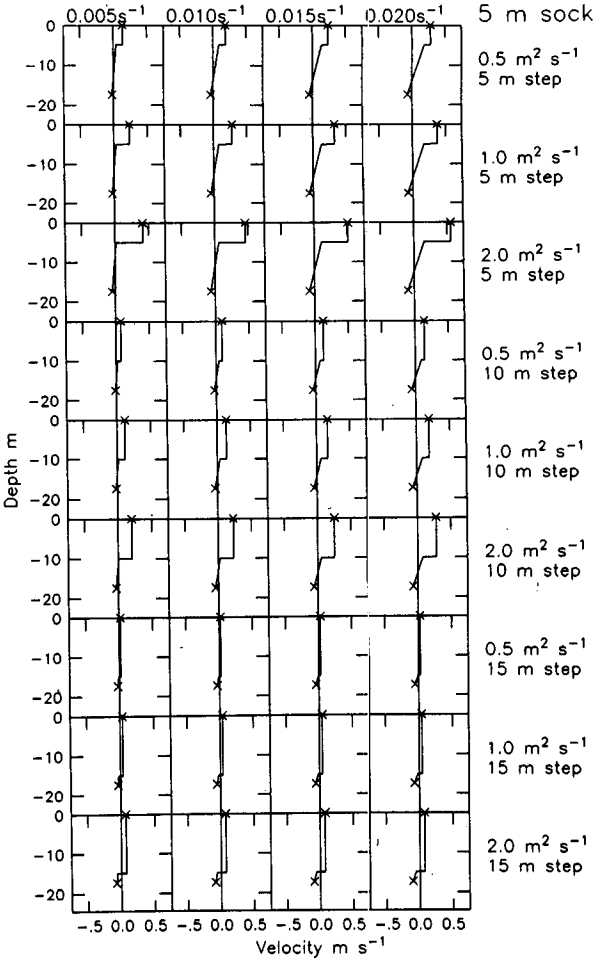

FIG. 8. The relative velocity profiles corresponding to the solutions in Table 1 and Fig. 7. The zero crossing in relative velocity is the depth of no slip. The top and bottom of the profile are marked with a cross.

lated at the fixed depth of 15 m. Since a drogue of finite length is drogued to a depth interval and not a fixed depth; unless otherwise noted we will be referring to ⟨slip⟩ when we discuss the slip results. These solutions were calculated using 2.5 cm segment lengths and a tolerance of 10^{-8} N on the residual force balance, corresponding to a rise accuracy of 2.5 cm and a slip accuracy of 0.1 cm s^{-1}.

Table 1 summarizes the results for a 5 m sock with a 12.5 m tether. For fixed step and momentum values, it is generally true that the slip increases with increasing linear shear. If momentum is kept fixed and the step size is increased (or equivalently, the velocity difference across the step is decreased), the slip decreases. As the momentum (velocity difference) is increased for a fixed step size, the slip increases. For the 5 m sock, the velocity step is confined to the tether except for the largest step size. The vertical rise of the drogue is less than 0.13 m.

The horizontal and vertical displacement of the tether and drogue from a straight vertical configuration is shown in Fig. 7; each diagram corresponds to a numerical solution in Table 1. The relative velocity profile for these numerical solutions is shown in Fig. 8. The zero crossing in relative velocity is the depth of zero slip and of zero horizontal force. Thus, the difference between the depth of zero slip and 15 m is a graphic representation of how well the drogue measures the water velocity at 15 m. The horizontal and vertical displacement is a graphic representation of the rise of the tether and drogue. There will be no horizontal displacement unless there is vertical rise. Most of the solutions for the 5 m sock have negligible horizontal displacement since there is very little rise. The horizontal displacement has been plotted with a 2:1 horizontal: vertical distortion to enable the reader to distinguish

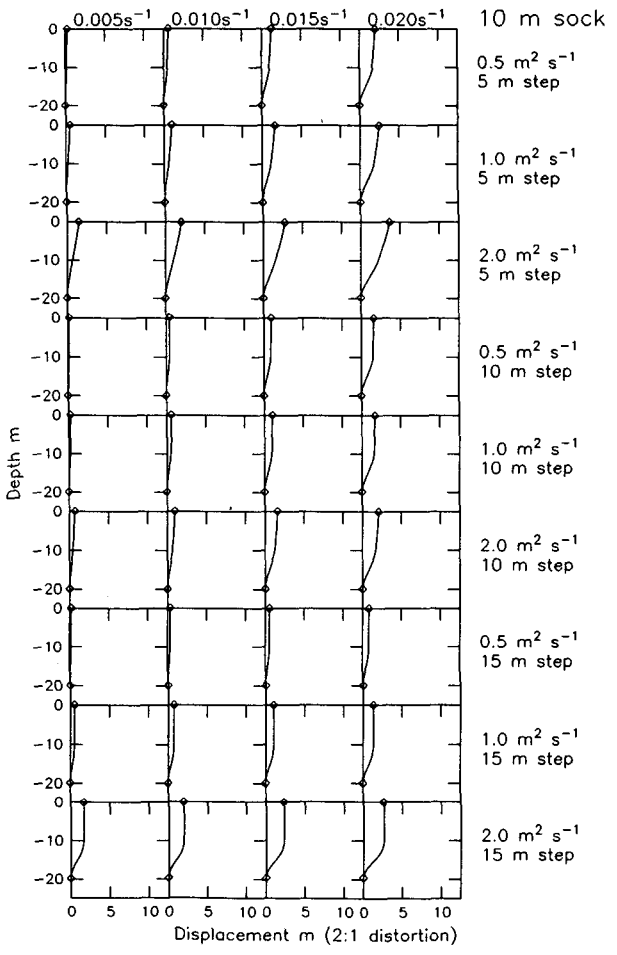

FIG. 9. Shape (horizontal versus vertical displacement from straight vertical) of the 10 m sock corresponding to the solutions in Table 2. Each column corresponds to a fixed value of linear shear. Each row corresponds to a fixed step size and momentum value. The first row corresponds to the first group of solutions in Table 2, etc. The horizontal to vertical distortion is 2:1. The top and bottom of the drogue are marked by open symbols.

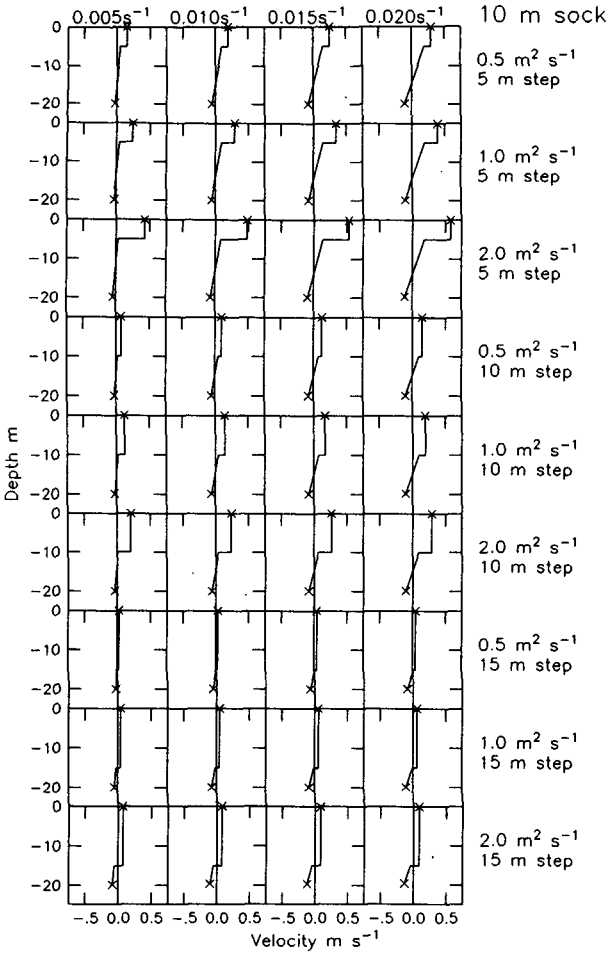

FIG. 10. The relative velocity profiles corresponding to the solutions in Table 2 and Fig. 9. The zero crossing in relative velocity is the depth of no slip. The top and bottom of the profile are marked with a cross.

between shapes for different velocity profiles. For step sizes of 5 and 10 m, the tether and drogue have similar tilts. For the largest step size, the tether hangs vertically (it lies totally within the step) and the horizontal displacement occurs over the length of the drogue. The values of the slip are smallest for the largest step size since when the tether hangs vertically it has minimal horizontal drag.

The relative velocity profiles for the extreme "worst case" shear are found in the third row of Fig. 8, corresponding to a step of 5 m and a velocity change of 0.4 m s^{-1} across the step. For this row (and for the whole table), the largest slip (0.044 m s^{-1}) occurs for the largest linear shear value (0.02 s^{-1}). Examining the relative velocity profiles for this row of solutions, we find that the depth of no slip deepens (moves closer to 15 m) as the shear increases, but due to the increasing shear, the relative velocity at 15 m is still larger at the largest shear value despite the deepening of the depth of no slip.

Table 2 summarizes the results for a 10 m sock with a 10 m tether. This sock resulted in the smallest calculated slips, with 28 out of 36 slip values less than 0.01 m s^{-1}. The largest slip was 0.023 m s^{-1}, corresponding to a 5 m step, momentum value of 2 $m^2 s^{-1}$, and a linear shear of 0.005 s^{-1}. Figure 9 shows the solution shapes of the tether and drogue corresponding to the numerical solutions in Table 2. The relative velocity profiles corresponding to the solutions in Fig. 9 are shown in Fig. 10. The largest slip occurred for the smallest step (largest velocity difference across the step) but for the weakest linear shear, in contrast to the 5 m sock. The depth of no slip is close enough to 15 m for the largest linear shear value such that the drogue slips somewhat less than for the case of the smallest linear shear. There is more horizontal displacement (and vertical rise) of the 10 m sock than we saw previously

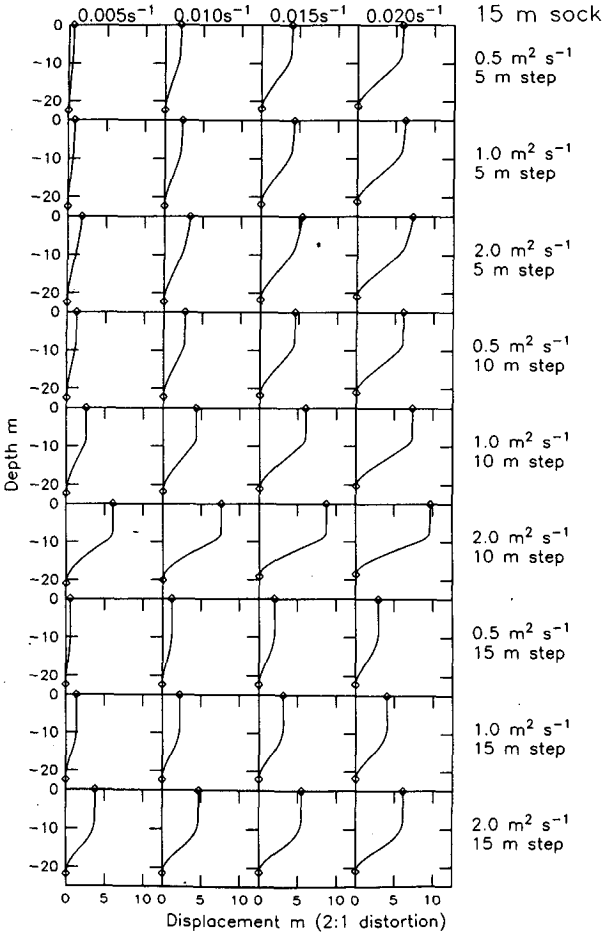

FIG. 11. Shape (horizontal versus vertical displacement from straight vertical) of the 15 m sock corresponding to the solutions in Table 3. Each column corresponds to a fixed value of linear shear. Each row corresponds to a fixed step size and momentum value. The first row corresponds to the first group of solutions in Table 3, etc. The horizontal to vertical distortion is 2:1. The top and bottom of the drogue are marked by open symbols.

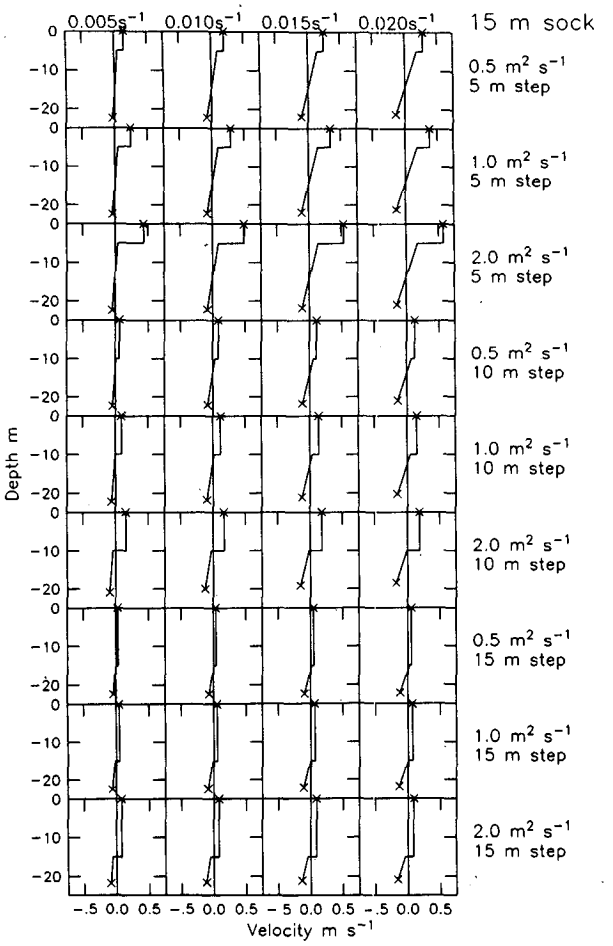

FIG. 12. The relative velocity profiles corresponding to the solutions in Table 3 and Fig. 11. The zero crossing in relative velocity is the depth of no slip. The top and bottom of the profile are marked with a cross.

for the 5 m sock. Also, there is a change in angle between the drogue and tether. The tether hangs more vertically than the drogue in these solutions, indicating more horizontal drag on the drogue element and thus better water following properties in the depth interval of interest.

Table 3 summarizes the results for a 15 m sock with a 7.5 m tether. Again, we find that the slip increases with increasing shear. The step size of 10 m includes approximately 2.5 m of sock, as evidenced in the large increase in both slip and vertical rise. If we averaged over the drogue length (15 m) rather than a fixed depth interval (5 m) then the slips would be smaller. However, if we are interested in testing this drogue design as a device to measure the 5 m averaged flow centered at 15 m, then the 5 m average is the appropriate definition of slip to use. A large proportion of the slip for the 10 m step case derives from the rise of the drogue; the drogue rises by as much as 4 m. The drogue rise in a step profile is much greater than that seen in a linear shear flow. The rise is actually reduced when the step includes more of the sock (15 m step).

The shapes of the 15 m drogue corresponding to the numerical solutions in Table 3 are displayed in Fig. 11. The corresponding relative velocity profiles are displayed in Fig. 12. The horizontal distortion is particularly deceptive in Fig. 11. As vertical rise is converted into horizontal displacement, the drifter appears to get longer but actually gets stretched by the plot scaling. The tether remains nearly vertical for most of these solutions. The slip of the 15 m drogue results from its length; it is depth averaging the flow over a larger interval than the one prescribed. This set of numerical calculations yields the largest number of slip velocities greater than 0.01 m s^{-1}. The slips are both positive and negative; the depth of no slip lies both above and below 15 m (Fig. 12). All slips were negative for the

5 m sock. Slips of both signs were calculated for the 10 m sock.

In summary, the performance characteristics of 3 drogues designed to measure the water velocity at 15 m in an upper-ocean mixed-layer jet overlying a linear shear were compared. The velocity profiles were chosen in the spirit of designing for a "worst case" shear. The best overall results for the cases considered were for the 10 m drogue (aspect ratio unity). The drogue was long enough to measure the averaged flow but not so long that its tilt and rise contributed to the slip. Although not shown, these calculations were made for other end weights. Slips in all cases were reduced by adding more end weight. The rise of the 15 m sock was also further reduced by adding more weight. Calculations that neglected drag on the surface float were also made; reducing the drag on the surface float reduced the slip.

7. Conclusions

The aim of this study was to examine what parameter changes were most effective in reducing the slip of a flexible, weighted, drogued surface drifter. Although the simple model used cannot account for slip due to windage or the surface wave field, it can present a theoretical lower bound on the amount of slip to be expected for a given flow regime. The aim is to try to choose a design that minimizes this lower bound with the understanding that the actual slip will be greater than this amount.

Analytic solutions were derived for a simple 2 lumped mass holey sock drogue in a linear shear profile, in the limit of small deviations from a straight vertical configuration. In this limit, which requires a small drag-to-weight ratio, the slip scales linearly with velocity difference across the drogue. The slip normalized by the velocity difference is inversely proportional to the drag area ratio of drogue to tether. The aspect ratio of tether length to drogue length for these calculations was unity. Numerical computations using a static equilibrium finite elements numerical model confirmed the functional dependence predicted by the simple analytic solution and provided least squares estimates of the dependences, in the limits considered. The best design for a linear shear is one that maximizes the drag area ratio of drogue to tether. However, due to the symmetry of the relative velocity profile in the case of linear shear, a simple rope drogue of the appropriate length to experience no horizontal force at the desired depth will also work. The design problem that really needs to be addressed is that of designing for an unknown vertical distribution of shear that may contain biases (asymmetries).

The numerical model was not restricted to either linear shear profiles or the parameter ranges of the analytic solution. The final computations examined the behavior of three different configurations of holey sock drifters in a series of velocity profiles chosen to model a surface diurnal jet overlying a linear shear. Drag on a surface buoy assumed to be submerged 100% of the time was included in these calculations, which were meant to be "worst case" realizations. The asymmetry of the velocity profile resulted in larger slips than in the case of symmetric linear shear. The results of the linear shear calculation also apply to these results: slip is proportional to the shear and inversely proportional to the drag ratio of the drogue to the tether. A critical parameter was the choice of the aspect ratio of tether to drogue length in the specified velocity profile. Choosing a drogue length to vertically average over the depth interval of interest, yet deep enough below the jet to minimize its vertical rise, was found to minimize the calculated slip.

The sensitivity of the calculation to the specific choice of velocity profile when the profile is not symmetric makes it difficult to optimize a surface drifter for all conditions. This suggests a real need to monitor the flow relative to the drifter, such as including a current measuring device, as part of the design of the surface drifter. Direct measurement of the slip, as well as calibration of surface drifters under various wind and wave conditions, are crucial to the understanding of the behavior of surface drifters and the interpretation of drifter measurements.

Acknowledgments. We thank A. J. Harding for useful discussions. This work was supported by the National Science Foundation under Contract OCE-8S17376 as part of the TOGA program.

REFERENCES

Berteaux, H. O., 1976: *Buoy Engineering.* Wiley and Sons, 314 pp.

Chereskin, T. K., J. N. Moum, P. J. Stabeno, D. R. Caldwell, C. A. Paulson, L. A. Regier and D. Halpern, 1986: Fine-scale variability at 140°W in the equatorial Pacific. *J. Geophys. Res.*, **91,** 12 887–12 897.

Chhabra, N. K., 1976: Mooring mechanics—a comprehensive computer study. Volume II: Three-dimensional dynamic analysis of moored and drifting buoy systems, The Charles Stark Draper Lab., Inc., Rep. CSDL-R-1066, 277 pp.

——, J. M. Dahlen and J. R. Scholten, 1987: Calibration of the Draper Laboratory Low Cost Drifter (LCD). The Charles Stark Draper Lab., Inc., Rep. CSDL-R-1906, 137 pp.

Dahlen, J. M., 1986: The Draper LCD: A calibrated, low cost Lagrangian drifter. The Charles Stark Draper Laboratory, Inc., Rep. CSDL-P-2670, 14 pp.

Niiler, P. P., R. E. Davis and H. J. White, 1987: Water-following characteristics of a mixed-layer drifter. *Deep-Sea Res.*, **34,** 1867–1881.

Press, W. H., B. P. Flannery, S. A. Teukolsky and W. T. Vettering, 1986: *Numerical Recipes.* Cambridge University Press, 818 pp.